Open Access

SCHOLARENA

Journal of Materials Science and Metallurgy

RESEARCH ARTICLE

ISSN: 2768-1912

Structural Evolution and Thermal Stability of FeCoNiMn (Al, Ti, Sn) High-Entropy Alloy Processed by High-Energy Ball Milling

Ben Ammar Cherif*

Laboratory of Inorganic Chemistry, LR17-ES-07, Faculty of Science, University of Sfax, Sfax 3018, Tunisia

***Corresponding Author:** Ben Ammar Cherif, Laboratory of Inorganic Chemistry, LR17-ES-07, Faculty of Science, University of Sfax, Sfax 3018, Tunisia, E-mail: cherif.bnamar@gmail.com

Citation: Ben Ammar Cherif (2026) Structural Evolution and Thermal Stability of FeCoNiMn (Al, Ti, Sn) High-Entropy Alloy Processed by High-Energy Ball Milling, J Mater Sci Metall 7 (1): 101

Abstract

The $Fe_{30}Co_{20}Ni_{20}Mn_{20}$ $(Al,Ti,Sn)_{10}$ high-entropy alloy was synthesised by high-energy ball milling, and its structural, microstructural, and thermal evolution was investigated as a function of milling time. X-ray diffraction combined with Rietveld refinement reveals a progressive dissolution of the constituent elements into a nanocrystalline face-centred cubic (FCC) solid solution between 10 and 50 h of milling. At longer milling times, weak diffraction peaks associated with Al- and Ti-rich intermetallic phases begin to emerge, indicating the onset of local chemical ordering or precipitation. Scanning electron microscopy shows pronounced particle refinement accompanied by repeated cold welding and fracture, leading to powders predominantly below 50 μm with occasional agglomerates reaching larger sizes. This evolution reflects the strong competition between plastic deformation and brittle fragmentation during mechanical alloying.

Differential scanning calorimetry reveals two dominant thermal events at approximately 490 °C and 665 °C. The first is attributed to recovery and relaxation of stored lattice defects, while the second is associated with ordering reactions and/or the formation of intermetallic compounds. Overall, the results highlight the critical role of Al, Ti, and Sn additions in controlling phase stability, defect accumulation, and thermal response in Fe-based high-entropy alloys, providing insights for tailoring nanostructured HEAs via mechanical alloying.

Keywords: High-entropy alloys; mechanical alloying; X-ray diffraction; nanostructure; thermal analysis; DSC; FCC solid solution

1. Introduction

High-entropy alloys (HEAs), first proposed by Yeh et al. [1], represent a new class of multi-principal element materials composed of five or more elements in near-equiatomic or concentrated compositions. Unlike conventional alloys based on one principal element, HEAs are designed to maximize configurational entropy, which can stabilize simple solid-solution phases such as face-centred cubic (FCC), body-centred cubic (BCC), or dual-phase (FCC + BCC) structures. In some cases, metastable or amorphous phases may also form depending on processing conditions and chemical complexity [2]. Owing to their unique compositional flexibility, HEAs often exhibit a combination of attractive properties, including high strength, good thermal stability, wear resistance, and in some systems, soft magnetic behaviour. These properties have made them promising candidates for structural and functional applications under extreme environments [3].

The mechanical alloying process facilitates the formation of HEAs primarily through the influence of entropy, which drives the mixing reaction. This process significantly lowers the free Gibbs energy ($\Delta G_{mix} = \Delta H_{mix} - T\,\Delta S_{mix}$), even at relatively low temperatures. As a result, super-saturated solid solutions are often produced instead of ordered phases, necessitating high temperatures for their formation. For example, the binary Fe–Co alloy is known for its soft magnetic properties, while the addition of Ni to Fe improves both electrical resistivity and permeability [4].

High-entropy alloys (HEAs) have been synthesised through powder metallurgical processes, deposition techniques, and melting and casting methods [5]. The broad compositional range and intricate dimensions of HEAs are further enhanced by incorporating a nanocrystalline structure. Moreover, studies have shown that nanostructured HEAs exhibit excellent magnetic properties [6], improved thermal stability [7], and superior mechanical performance [8]. Mechanical alloying (MA) is a widely adopted method for producing nanoscale solid solution structures with unique properties, serving as an alternative to arc melting and traditional foundry techniques for creating high-entropy alloys [9,10]. MA offers the advantage of extended solid solubility even in systems that are typically immiscible, likely reflecting the prolonged diffusion times associated with the nanoscale size of the powder components before alloying. Consequently, MA enhances the phase stability of HEAs while also increasing their configurational entropy.

In recent years, the use of high-energy ball milling has significantly increased to produce materials with high entropy [11]. This surge in interest is this indicates the mechanical action of the balls on the powder during milling, which leads to the formation of a unique microstructure [11]. This unique microstructure endows the materials with crucial properties that are highly desirable for various advanced applications [12].

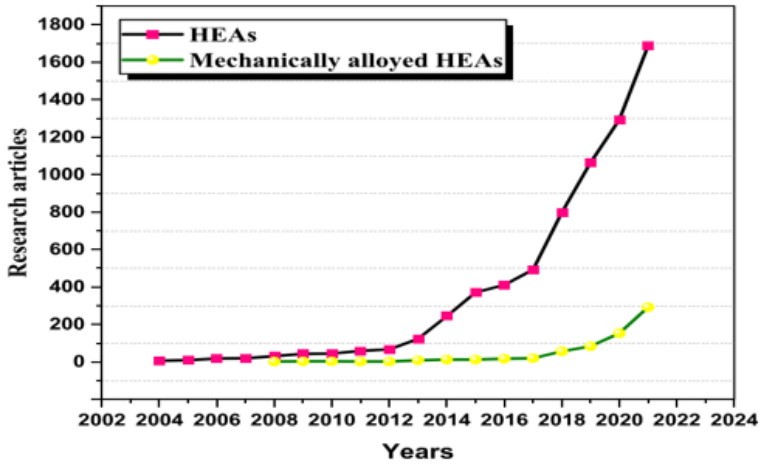

Figure 1: The progress of research articles pertaining to the synthesis of HEAs via MA [11]

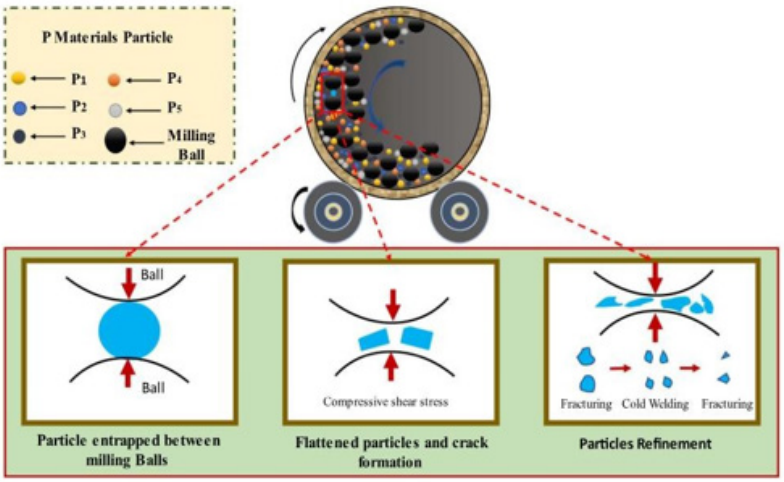

Figure 2: Planetary ball milling and different stages in MA [11]

Consequently, the ternary Fe–Co–Ni alloy has exhibited excellent soft magnetic characteristics, making it suitable for various technological applications, including magnetic recording media and magnetic fluids [13, 14].

The present study investigates the effect of Al, Ti and Sn additions on the Fe–Co–Ni–Mn system through the synthesis of a $Fe_{30}Co_{20}Ni_{20}Mn_{20}$ $(Al,Ti,Sn)_{10}$ high-entropy alloy by high-energy ball milling and the evaluation of its structural, microstructural and thermal evolution.

HEAs based on FeCoNi

The majority of HEAs currently studied are based on the CoCrFeNi system with various additions or substitutions of elements such as Al, Ti, and Sn. The effect of different alloying elements on the microstructure and properties of this system is examined below.

a. Effect of Aluminum Addition

In metallic alloys, the addition of aluminum can significantly influence structural, microstructural, magnetic, and mechanical properties, especially in high-entropy alloys. Aluminum can alter the alloy's crystalline structure, thereby affecting its strength, ductility, and thermal stability. Additionally, aluminum can impact the magnetic properties of the alloy, which can have implications for its electrical conductivity and performance in magnetic applications.

Effect of Al on Microstructure

The influence of aluminium addition directs microstructural characteristics towards the formation of intermetallic phases, resulting in impressive improvements in mechanical properties, especially in refractory applications, while also reducing alloy density [15]. The addition of Al promotes the formation of BCC phases [16,17], and studies on microstructure influence focus on the effect of these properties on enhancing wear resistance, notably through the formation of a protective oxide film [16]. The most commonly studied alloys include those with varying Al content in this base system (CoCrFeNi) with Ti and/or Cu also present. The variation in Al content is widely studied because it has a clear effect on the resulting crystallographic phase. As mentioned in the section, with increasing Al, the crystallographic structure changes from a complete FCC structure to a combination of FCC + BCC structures, and with sufficient Al, a complete BCC structure is observed [18].

Effect of Al on Mechanical Properties

The introduction of aluminium into high-entropy alloys (HEAs) brings about notable changes in their mechanical properties [19]. Indeed, this addition can impart greater strength to HEAs but at the expense of their ability to deform without fracturing. According to recent studies, such as that conducted by Zhang et al. (2021) [20], the addition of aluminium enhances the tensile strength of HEAs but decreases their ductility. Similarly, research by Ye et al. (2020) [21] reveals that the incorporation of aluminium can improve the corrosion resistance of HEAs while reducing their stress rupture strength. These findings underscore the crucial importance of aluminium addition in seeking an optimal balance between the strength and flexibility of HEAs, depending on the specific requirements of each application.

Effect of Al on Magnetic Properties of High-Entropy Alloys

The addition of aluminium (Al) to high-entropy alloys can influence the nature of their magnetic properties. Studies, such as that by Li et al. (2018) [22] on FeCoCrNiAl alloys, have shown an increase in magnetization, suggesting potential for magnetic applications. Furthermore, increasing aluminium concentration can contribute to an increase in magnetic saturation (Ms), indicating an enhanced ability of the material to maintain a strong magnetic moment. However, it is important to note that the effect of Al on magnetic hardness (Hc) may vary depending on the overall alloy composition and heat treatment conditions.

b. Effect of Titanium Addition

The addition of titanium to metallic alloys offers significant advantages, such as its lightweight nature, corrosion resistance, and heat resistance. These properties make titanium an ideal choice for reinforcing alloys, particularly in high-entropy alloys, where it can enhance overall alloy performance.

Effect of Ti on Microstructure

The controlled introduction of titanium (Ti) into high-entropy alloys (HEAs) is of increasing interest due to its significant influence on the microstructure of these materials. Previous research, such as that conducted by Zhang et al. [23], has demonstrated that the incorporation of Ti can significantly modulate phase formation and the distribution of constituent elements within HEAs. For example, increasing Ti content often promotes the precipitation of intermetallic phases, resulting in discernible changes in texture and stability of the microstructure. This observation is crucial in understanding grain growth mechanisms and the morphology of phases present in HEAs. These microstructural aspects are essential for evaluating the mechanical and thermal properties of alloys and for designing HEAs with optimized performance.

Effect of Ti Addition on Mechanical Properties

The addition of titanium to high-entropy alloys strengthens these materials by promoting the formation of dispersed intermetallic phases, making them more resistant to traction. For example, in a study by Chen et al. in 2020, the incorporation of titanium into a FeCrNiMn alloy significantly improved its tensile strength [24]. Additionally, titanium helps increase the hardness of these alloys by promoting the formation of hard and dispersed phases, as observed in a study by Tong et al. in 2019 on a FeCoCrNi alloy [25]. Finally, titanium also enhances the toughness of high-entropy alloys by promoting the formation of metastable phases and refining the microstructure, as demonstrated by Li et al. in 2018 in their study on a FeCoCrNiCu alloy [26]. These studies highlight the mechanical advantages of adding titanium to these alloys.

Effect of Ti on Magnetic Properties of High-Entropy Alloys

The incorporation of titanium (Ti) can also affect the magnetic properties of high-entropy alloys. For example, in studies on Fe-

CoCrNiTi alloys, a decrease in magnetization and coercivity (Hc) has been observed, suggesting a suppressive effect on the "hard" nature of alloys. However, specific values of Hc and Ms may vary depending on the titanium concentration and other alloying elements. A decrease in Hc may indicate a reduction in the material's ability to maintain an external magnetic field, while a decrease in Ms may reflect a reduction in magnetic saturation [23].

c. Effect of Tin Addition

The addition effect, also known as the alloying effect, refers to changes in the physical and chemical properties of a metal when alloyed with another metal or metallic alloys. In the case of high-entropy alloys, the presence of tin can have several effects. It can stabilize phases and guide phase formation along well-defined pathways with precise control. Additionally, it can enhance corrosion resistance and mechanical properties such as tensile strength and hardness.

Influence on Microstructural and Mechanical Properties

The addition of Sn to high-entropy alloys modifies their microstructure and mechanical properties. At low Sn content, the crystalline structure remains FCC, but as the amount of Sn increases, intermetallic compounds appear. This transition results in improved alloy strength and ductility. In summary, the incorporation of Sn strengthens high-entropy alloys, thereby improving their robustness and ductility [27]. The use of high-entropy alloys in extreme environments requires exceptional corrosion resistance properties. The addition of Sn to CoCrFeNiSn alloys appears to play a crucial role in enhancing this resistance, especially under chloride attack. By forming stable protective films of Cr2O3 and SnO2 on the alloy surface, and promoting the formation of beneficial phases such as Ni-Sn, this addition of Sn offers promising prospects for applications where corrosion protection is essential, such as marine environments [28].

Effect of Sn on Magnetic Properties of High-Entropy Alloys

The addition of tin (Sn) can also alter the magnetic properties of high-entropy alloys. For example, studies on FeCoCrNiSn alloys have shown a decrease in magnetization and coercivity (Hc), suggesting a trend towards a soft nature of the material. However, the precise mechanisms behind these observations and how they interact with other alloying elements require further study for a comprehensive understanding of the magnetic properties of these alloys [29].

Study of the Formation and Stability of High-Entropy Alloys

The stability of compounds formed during mechanical alloying can be hypothesized based on the study of parameters related to the electronic structure of each starting element, which may influence the phases formed, such as Valence Electron Concentration (VEC) Valence Electron Concentration (VEC) quantifies the electrons per formula unit and significantly influences the structural, thermodynamic, and mechanical properties of binary and ternary compounds. In high-entropy alloys, VEC predicts phase stability and structural transitions. It is calculated using the equation:

$$VEC = \sum_{i=0}^{n} c_i (VEC)_I$$

Where Ci represents the molar quantity of the i-th component and (VEC)i denotes the valence electron concentration of the i-th component.

Specifically, VEC < 6.67 favors stability in body-centred cubic (BCC) structures, VEC > 8 favors face-centred cubic (FCC) structures, and 6.87 < VEC < 8 reflects stable mixed phases [30]. The objective of this study is to produce FeCoNiMn (Al,Ti,Sn) high-entropy alloys (HEAs) and analyses how milling duration during mechanical alloying affects their properties. The investigation utilizes X-ray diffraction (XRD) and scanning electron microscopy (SEM) combined with energy-dispersive X-ray spectros-

copy (EDS) to examine microstructure and differential scanning calorimetry (DSC) to study phase formation and thermal properties. The alloy samples are mechanically alloyed for 100 hours to explore these aspects comprehensively.

2. Experimental procedure

Elemental powders of Fe, Co, Ni, Mn, Al, Ti, and Sn with a purity higher than 99.5% and particle sizes ≤ 30 μm (Alfa Aesar) were used as starting materials. The powders were weighed to obtain the nominal composition $Fe_{30}Co_{20}Ni_{20}Mn_{20}(Al,Ti,Sn)_{10}$ (at.%) and mechanically alloyed using a high-energy planetary ball mill (Fritsch Pulverisette P7, Fritsch GmbH, Germany) under an argon atmosphere to minimise oxidation.

Mechanical alloying was performed in a hardened steel vial at a rotational speed of 600 rpm. The ball-to-powder weight ratio was fixed at 0.47. To limit excessive cold welding and powder adhesion to the vial walls, a discontinuous milling режим was adopted, consisting of alternating cycles of 10 min milling followed by 5 min rest. Powders were collected after selected milling times up to 100 h to investigate the evolution of structure and properties as a function of processing duration.

Phase identification and structural analysis were performed by X-ray diffraction (XRD) using Cu Kα radiation on a Siemens D500 diffractometer operating in Bragg–Brentano (θ–2θ) geometry. The diffraction data were analysed using full-pattern Rietveld refinement to quantify phase evolution, lattice parameter variation, and crystallite size reduction [32]. The morphology and particle evolution were examined using scanning electron microscopy (SEM, ZEISS DSM960A) operated in secondary electron mode at an accelerating voltage of 15 kV. Elemental composition was qualitatively analysed using energy-dispersive X-ray spectroscopy (EDS) (TESCAN VEGA system). Particle size distribution was evaluated using ImageJ software based on SEM micrographs.

Thermal behaviour was investigated by differential scanning calorimetry (DSC) using a Mettler Toledo DSC 822 system. Measurements were carried out from room temperature to 700 °C at a heating rate of 10 °C/min under continuous argon flow to prevent oxidation. Alumina crucibles were used for reference and sample holders. The heat flow signal was recorded as a function of temperature to identify phase transformations, recovery processes, and possible ordering reactions during heating [33].

3. Results and discussion

3.1. SEM-analysis

The SEM analysis of the mechanically alloyed $Fe_{30}Co_{20}Ni_{20}Mn_{20}$ $(Al,Ti,Sn)_{10}$ powder mixture, observed at different magnifications (×500, ×2500, and ×25000 corresponding to 200 μm, 50 μm, and 5 μm scales, respectively) (fig. 3), reveals a heterogeneous particle morphology. Most particles are smaller than 50 μm, while larger cold-welded agglomerates reaching approximately 150 μm are also observed. The particle morphology evolves from spherical to polygonal shapes, reflecting the combined effects of repeated plastic deformation, cold welding, and fracture during high-energy ball milling. These competing mechanisms are characteristic of mechanically alloyed systems and govern the steady-state microstructural evolution of the powder.

The addition of Al and Ti, which exhibit relatively high ductility in the early stages of milling, promotes plastic deformation and enhances cold-welding events between particles. In contrast, harder constituents contribute to repeated fracture, leading to progressive particle refinement [34,35]. Sn also participates in the microstructural evolution by influencing local deformation heterogeneity [12]. With increasing milling time, repeated deformation induces severe work hardening and the accumulation of crystallographic defects, including dislocations and lattice distortions. This leads to progressive particle refinement and the development of a highly strained microstructure, which is a precursor for the formation of a nanocrystalline solid solution.

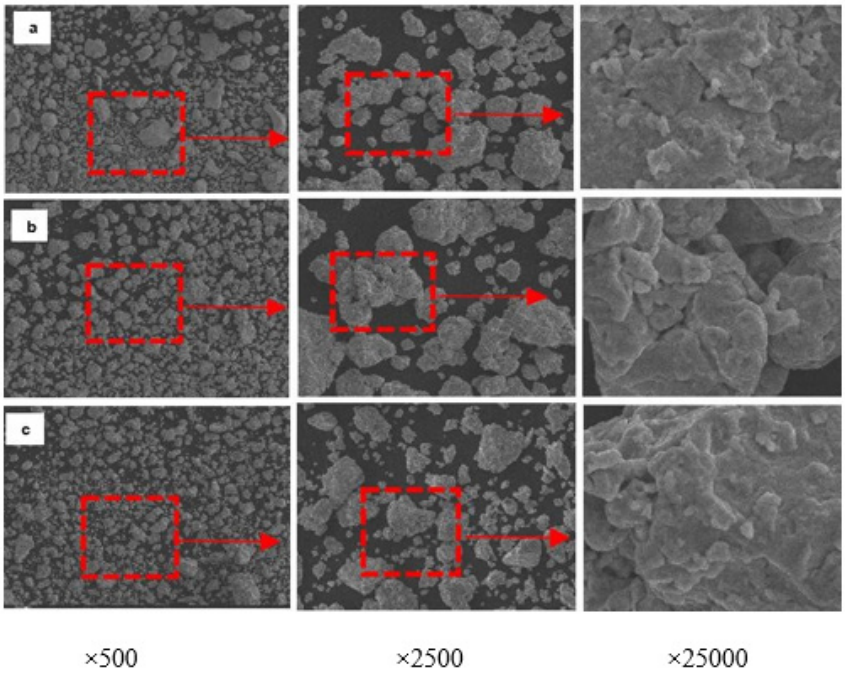

Figure 3: SEM photos of the MA $Fe_{30}Co_{20}Ni_{20}Mn_{20}$ $(Al,Ti,Sn)_{10}$ powder mixture obtained after various MA times: (a) 4 h, (b) 50 h, and (c) 100 h

The morphological evolution of mechanically alloyed (MA) powder mixtures after 100 hours of milling reveals distinctive changes among $Fe_{30}Co_{20}Ni_{20}Mn_{20}$ $(Al,Ti,Sn)_{10}$ (Fig.4a), Fe30Co20Ni20Mn20Al10 (Fig. 4b), and $Fe_{30}Co_{20}Ni_{20}Mn_{20}$ $(Al,Ti,Sn)_{10}$ (Fig. 4c), building upon previous studies conducted on $Fe_{30}Co_{20}Ni_{20}Mn_{20}$ $(Al,Ti,Sn)_{10}$ [12] and $Fe_{30}Co_{20}Ni_{20}Mn_{20}$ $(Al,Ti,Sn)_{10}$ [31].

The SEM images at 500x magnification depict unique microstructural characteristics for each alloy composition. $Fe_{30}Co_{20}Ni_{20}Mn_{20}$ $(Al,Ti,Sn)_{10}$ (scale of 60μm) exhibits a morphology featuring fine particles and clusters up to 160 μm, attributed to intense fracturing and a dense network of crystallographic defects facilitated by aluminium and titanium. In contrast, $Fe_{30}Co_{20}Ni_{20}Mn_{20}$ $(Al,Ti,Sn)_{10}$ (scale of 60μm) shows severely deformed aluminium particles bonding with harder counterparts, forming larger agglomerates through cold welding, alongside the creation of fine particles this indicates vigorous fracturing and the formation of supersaturated solid solutions [12]. Meanwhile, $Fe_{30}Co_{20}Ni_{20}Mn_{20}$ $(Al,Ti,Sn)_{10}$ (scale of 60μm) displays a refined microstructure characterized by very fine particles, indicative of extensive particle fracture and increased hardness from the dissolution of metallic elements to form supersaturated solid solutions [34, 35]. These findings underscore the significant influence of alloy composition on the morphological variations observed after prolonged milling, highlighting distinct mechanisms of microstructural evolution and providing valuable insights into the effects of composition on mechanical alloying processes.

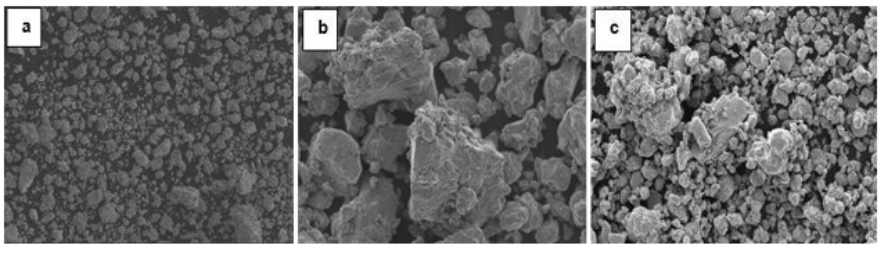

Figure 4: SEM photos of the MA powders mixtures obtained after MA time: 100 h, a) $Fe_{30}Co_{20}Ni_{20}Mn_{20}$ $(Al,Ti,Sn)_{10}$ 10 b) $Fe_{30}Co_{20}Ni_{20}Mn_{20}A_{l10}$, c)) $Fe_{30}Co_{20}Ni_{20}Mn_{20}Ti_{10}$

3.2. XRD-analysis

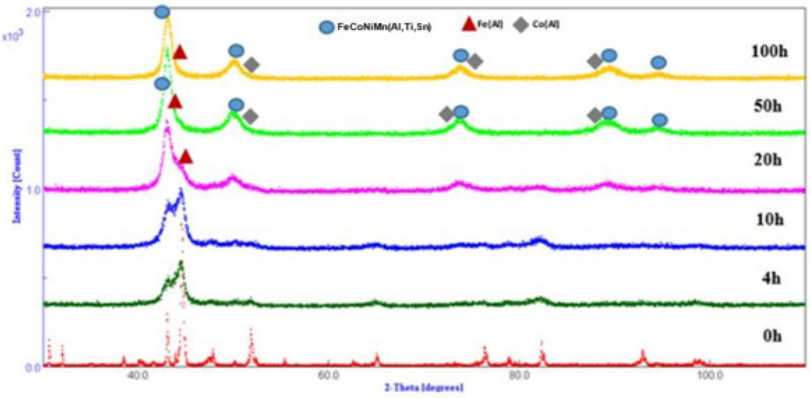

Figure 5: XRD patterns of the) $Fe_{30}Co_{20}Ni_{20}Mn_{20}$ powdered specimens collected after selected MA times.

The figure shows the XRD diagrams of) $Fe_{30}Co_{20}Ni_{20}Mn_{20}$ HEA powders after different milling times. All characteristic peaks of elemental powders can be observed in the XRD pattern of the unmilled powder. There is CC-Fe (Im-3m ; a0=2,8667(1) Å), HCP-Co (P63/mmc ; a0=2,5071(1) Å et c=4,0713(1) Å), CFC-Ni (Fm-3m ; a0=3,5260(1) Å), CC-Mn (I-43m ; a0=8,9125 (1) Å and CFC-Al (Fm-3m ; a0=4,0478(4) Å. HCP-Ti (P63/mmc; a = 2.9064(1) Å and c=4.6667(1) Å) and Tetra-Sn (P4/nmm; a = 5.87(1) Å and c=3.18(1) Å). The high-entropy alloy) $Fe_{30}Co_{20}Ni_{20}Mn_{20}$ undergoes significant structural evolution as a function of mechanical milling time. The X-ray diffraction pattern of the 100 h milled sample exhibits main reflections at 43.12°, 50.04°, and 69.28° (2θ), corresponding to the (111), (200), and (220) planes of an FCC solid solution.

During the first 10 h of milling, diffraction patterns reveal distinct peaks associated with the elemental constituents, indicating a multiphase structure. Between 10 and 50 h, progressive peak broadening is observed, reflecting the gradual dissolution of Fe, Co, Ni, Mn, Al, Ti, and Sn into a supersaturated FCC solid solution. This transformation is driven by severe plastic deformation and enhanced atomic mixing induced by repeated cold welding and fracture events. From 50 to 100 h, a well-developed FCC Fe(Co,Ni,Mn) solid solution is formed, characterized by pronounced peak broadening, which is attributed to significant grain refinement down to the nanometric scale and high microstrain levels associated with defect accumulation [36]. Peak broadening therefore results from the combined effects of crystallite size reduction and lattice strain. Weak diffraction features observed at extended milling times suggest the possible formation of Al- and Ti-rich ordered clusters or intermetallic compounds. However, their low intensity reflects that these phases remain minor compared to the dominant FCC matrix. A slight increase in their intensity between 50 and 100 h may be associated with local compositional fluctuations and partial saturation of the solid solution.

The progressive refinement of crystallites during milling leads to a substantial increase in grain boundary volume fraction, resulting in significant storage of strain energy within the nanocrystalline structure. This stored energy, together with high defect density and lattice distortion, enhances atomic mobility and facilitates further solid solution formation [36, 37]. In addition, nanoscale lattice distortion induced by severe plastic deformation contributes to improved solubility of alloying elements. The microstructural evolution is therefore characterized by continuous grain refinement and progressive accumulation of crystalline defects such as dislocations and stacking faults, particularly between 10 and 50 h, reaching a maximum level between 50 and 100 h, which is responsible for the observed diffraction peak broadening.

Overall, the structural evolution of) $Fe_{30}Co_{20}Ni_{20}Mn_{20}$ is governed by the formation of a stable FCC solid solution enriched in Fe, Co, and Ni, while minor residual chemical heterogeneities may lead to localized Al- and Ti-rich ordering or intermetallic

formation. The continuous reduction in grain size and increase in defect density are typical features of intensive mechanical alloying processes [36, 37].

3.3. DSC-analysis

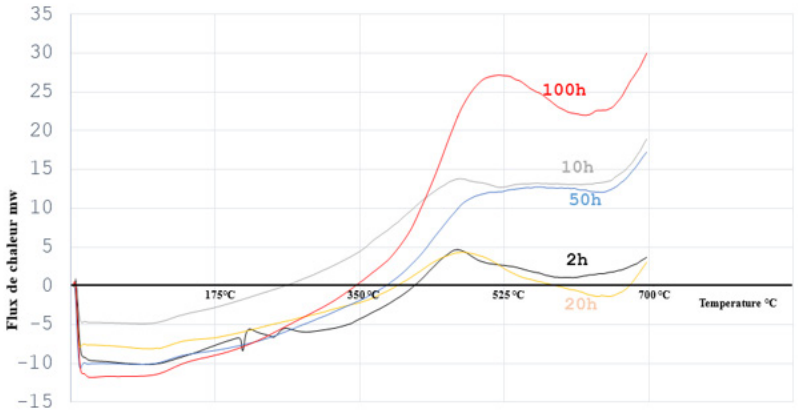

Figure 6: DSC curves of the) $Fe_{30}Co_{20}Ni_{20}Mn_{20}$ powdered specimens collected after selected MA times.

The Differential Scanning Calorimetry (DSC) analysis of the FeCoNiMnAlTiSn high-entropy alloy processed for different milling durations (2 h, 10 h, 20 h, 50 h, and 100 h) reveals a strong dependence of thermal response on the mechanical alloying history. The DSC curves, recorded between room temperature and 700 °C, exhibit distinct thermal events whose position and intensity evolve with milling time.For the 2 h milled sample, a weak thermal peak is observed around 280 °C, which can be associated with early-stage structural relaxation and minor rearrangement of the as-milled heterogeneous powder mixture. This reflects limited atomic mixing and a still incomplete development of a solid solution. At 10 h of milling, a more pronounced peak appears at approximately 420 °C, reflecting enhanced atomic mobility and the onset of significant structural reorganization. This behaviour is consistent with increased defect formation and the progressive development of chemically driven transformations within the mechanically activated system. For the 20 h sample, a thermal event is detected around 350 °C, suggesting ongoing structural evolution. The intermediate intensity of this peak reflects partial overlap between defect recovery and progressive phase reorganization, rather than a single well-defined transformation. At 50 h of milling, a broader and more pronounced exothermic response is observed near 455 °C. This feature is attributed to the release of accumulated lattice strain and internal stresses induced by severe plastic deformation. A weaker exothermic contribution is also detected, indicating overlapping recovery processes and progressive structural stabilization. These thermal events are consistent with continuous strain energy release and defect annihilation during heating [37].

For the 100 h milled sample, the thermal response becomes more complex and better defined. A dominant endothermic peak appears at approximately 490 °C, which is attributed to the recovery and relaxation of the high density of lattice defects accumulated during mechanical alloying, together with the onset of recrystallisation of the nanocrystalline FCC matrix. This event corresponds to the release of stored deformation energy within the heavily deformed structure. In addition, a secondary thermal event is observed near 665 °C, which may be associated with ordering reactions and/or precipitation of Al- and Ti-rich intermetallic phases from the supersaturated FCC solid solution. This reflects that prolonged milling enhances chemical metastability, enabling thermally activated decomposition processes at elevated temperatures [38]. The evolution of DSC signals with milling time demonstrates a clear transition from weak, diffuse thermal features at short milling durations to well-defined transformation peaks at extended milling. This evolution reflects the progressive increase in defect density, strain energy storage, and chemical supersaturation induced by mechanical alloying. The results highlight the strong influence of milling time on the thermal stability and phase transformation behaviour of the FeCoNiMnAlTiSn high-entropy alloy.

4. Phase Formation Hypothesis and Golden Ratio Considerations

The formation of phases in high-entropy alloys (HEAs) is governed by a complex interplay of atomic size, valence electron concentration (VEC), chemical interactions, and atomic packing effects. In the $Fe_{30}Co_{20}Ni_{20}Mn_{20}(Al,Ti,Sn)_{10}$ system, the differences in atomic radii (rFe = 126 pm, rCo = 125 pm, rNi = 124 pm, rMn = 127 pm, rAl = 143 pm, rTi = 147 pm, and rSn = 145 pm) generate significant local lattice distortions that promote the formation of a supersaturated FCC solid solution during mechanical alloying. In addition, local atomic rearrangements may favor the formation of highly packed configurations and contribute to the nucleation of minor Al- and Ti-rich phases. Such considerations are consistent with the efficient packing concepts commonly associated with the ideal HCP c/a ratio (~1.633) and related geometric principles [41].

The Golden Ratio ($\varphi \approx 1.618$), frequently discussed in quasicrystals, metallic glasses, and complex atomic arrangements, has been proposed in the literature as a possible geometric descriptor in complex atomic arrangements for interpreting local atomic organization in compositionally complex alloys [42, 44]. Although direct evidence of φ-governed ordering is not available in the present work, the proximity between φ and characteristic packing ratios suggests that local atomic configurations approaching efficient packing conditions may contribute to reducing local strain energy and enhancing structural stability during mechanical alloying.

The progressive formation of a nanocrystalline FCC matrix after 50–100 h of milling, together with the extensive peak broadening observed by XRD, reflects intense grain refinement and a high density of lattice defects. SEM observations reveal particle refinement, cold welding, and agglomerate formation resulting from repeated deformation and fracture events. These microstructural features suggest continuous atomic rearrangement processes that may be influenced by local geometric constraints arising from the significant atomic-size differences between Al, Ti, Sn and the transition-metal matrix elements [42, 44].

According to this hypothesis, mechanical alloying initially promotes the dissolution of the constituent elements into a supersaturated FCC solid solution, while local packing constraints may contribute to the subsequent formation of minor ordered or intermetallic regions enriched in Al and Ti. This interpretation is consistent with the XRD observations of peak broadening and weak secondary reflections, as well as the SEM evidence of refined particle clusters. Furthermore, the DSC thermal events observed near 490 °C and 665 °C may be associated with defect relaxation and subsequent ordering or precipitation phenomena, reflecting the progressive structural stabilization of the alloy during heating [39, 41 and 43].

Linking Experimental Observations to Geometric Packing Considerations

XRD Analysis: The FCC reflections (111), (200), and (220) dominate the diffraction patterns after prolonged milling. The pronounced peak broadening reflects nanocrystalline grain sizes and high defect densities. Weak reflections attributed to Al- and Ti-rich phases suggest local chemical and structural heterogeneities that may develop within highly distorted regions of the alloy [41, 43].

SEM Analysis: SEM images reveal particles smaller than 50 μm together with agglomerates reaching 150–160 μm, resulting from repeated fracture and cold-welding mechanisms. These observations indicate extensive microstructural reorganization during milling and support the existence of localized packing environments generated by severe plastic deformation [42, 44].

DSC Analysis: Thermal events observed near 490 °C and 665 °C are attributed to defect recovery, structural relaxation, and possible ordering or precipitation reactions. These transformations highlight the strong relationship between atomic arrangement, defect structure, and thermal stability in the mechanically alloyed HEA system [39, 41]

The combined effects of atomic-size mismatch, VEC, severe lattice distortion, and local geometric packing considerations provide a plausible framework for understanding the structural, microstructural, and thermal evolution of the $Fe_{30}Co_{20}Ni_{20}Mn_{20}(Al,Ti,Sn)_{10}$ alloy during high-energy ball milling. The possible role of geometric relationships related to the Golden Ratio should be regarded as a working hypothesis that warrants further investigation through advanced structural characterization and atomistic modelling.

5. Conclusion

The present work demonstrates that the $Fe_{30}Co_{20}Ni_{20}Mn_{20}(Al,Ti,Sn)_{10}$ high-entropy alloy develops a stable nanocrystalline FCC solid solution during high-energy ball milling. Its formation is governed by the combined effects of severe lattice distortion, progressive defect accumulation, and chemical complexity induced by Al, Ti, and Sn additions. Mechanical alloying promotes rapid elemental mixing and significant grain refinement, leading to a highly strained supersaturated FCC matrix. With increasing milling time, the system progressively approaches its solubility limits, resulting in the initial appearance of Al- and Ti-related ordering tendencies or incipient intermetallic formation. DSC analysis confirms that the mechanically activated structure stores a high level of strain energy, which is progressively released during heating through defect recovery and recrystallisation, followed by higher-temperature ordering and/or precipitation reactions. This clearly reflects the metastable nature of the milled solid solution and its strong dependence on defect structure.

Overall, the results highlight the effectiveness of mechanical alloying as a powerful route for tailoring the phase stability and thermal response of Fe-based high-entropy alloys. The studied system exhibits a high degree of structural tenability, making it a promising candidate for applications requiring controlled transformation behaviour and enhanced thermal stability.

References

1. Yeh JW, Chen SK, Lin SJ, Gan JY, Chin TS, et al. (2004) Nanostructured high-entropy alloys with multiple principal elements: novel alloy design concepts and outcomes. Adv Eng Mater 6: 299–303.

2. Schuh B, Mendez-Martin F, Völker B, George EP, Clemens H, et al. (2015) Mechanical properties, microstructure and thermal stability of nanocrystalline CoCrFeMnNi high entropy alloy. Acta Mater 96: 258–269.

3. Chen Z, Chen W, Wu B, Cao X, Liu L, et al. (2015) Effects of Co and Ti on microstructure and mechanical behaviour of Al0.75FeNiCrCo high entropy alloy. Mater Sci Eng A 648: 217–224.

4. Ammar CB, Khitouni N, Mbarek WB, Alsulami AH, Suñol JJ, et al. (2024) Properties of high-entropy Fe30Co20Ni20Mn20Al10 alloy produced by high-energy ball milling. Materials 17: 23.

5. Wu JM, Lin SJ, Yeh JW, Chen SK, Huang YS, et al. (2006) Adhesive wear behaviour of AlxCoCrCuFeNi high-entropy alloys. Wear 261: 513–519.

6. Tang Z, Gao MC, Diao H (2013) Aluminum alloying effects on lattice types and mechanical behaviour of HEAs. JOM 65: 1848–1858.

7. Zhang Y, Yang X, Zhang Y, Yi Y, Xu Y, et al. (2016) Microstructure and mechanical properties of AlxCoCrFeNi HEAs. Mater Sci Eng A 678: 183–190.

8. Zhang Y, Li Z, Tao N, Huang X, Chen Z, et al. (2021) Effect of Al content on AlxCoCrFeNi HEAs. Mater Sci Eng A 802: 140609.

9. Zhang Y, Zuo TT, Tang Z, Gao MC, Dahmen KA, et al. (2014) Microstructures and properties of HEAs. Prog Mater Sci 61: 1–93.

10. Ben Ammar CB, Khitouni N, Alshammari M, Alsawi A, Khitouni M, et al. (2024) Microstructural and magnetic characteristics of FeCoNiMnTi HEA. Metals 14: 1302.

11. Zhang K, Fu Z, Zhang J, Wang W, Lee S, et al. (2010) J Alloys Compd 495: 33–38.

12. Zhang B, Zhao R, Ren B, Jiang A, Chen C, et al. (2023) Mechanical alloying behaviour of HEA powders. Materials 16: 3179.

13. Shivam V, Basu J, Pandey VK (2018) Phase evolution in AlCoCrFeNi HEA. Adv Powder Technol 29: 2221–2230.

14. Caramarin S, Badea IC, Mosinoiu LF (2024) Structural particularities of HEAs. Appl Sci 14: 7576.

15. Kaloshkin S (2001) Physica B 299: 236–241.

16. Deguchi K (2012) Quantum critical state in magnetic quasicrystal. arXiv.17. Guo S, Liu C (2011) Phase stability in high-entropy alloys: formation of solid-solution phase or amorphous phase. Prog Nat Sci 21: 433–446.

17. Senkov ON, Wilks GB, Scott JM, Miracle DB (2011) Mechanical properties of Nb25Mo25Ta25W25 and V20Nb20Mo20Ta20W20 refractory high-entropy alloys. Intermetallics 19: 698–706.

18. Jiles D (1998) Introduction to Magnetism and Magnetic Materials. New York: Chapman and Hall/CRC.

19. Murty BS, Yeh JW, Ranganathan S (2014) High-Entropy Alloys. Butterworth-Heinemann.

20. Zhang Y, Zuo TT, Cheng YQ, Liaw PK (2013) High-entropy alloys with high saturation magnetization, electrical resistivity, and malleability. Sci Rep 3: 1455.

21. Praveen S, Basu J, Kashyap S, Kottada RS (2016) Exceptional resistance to grain growth in nanocrystalline CoCrFeNi high entropy alloy. J Alloys Compd 662: 361–366.

22. Suryanarayana C (2001) Mechanical alloying and milling. Prog Mater Sci 46: 1–184.

23. Kumar A (2022) A critical review on mechanically alloyed high-entropy alloys. Mater Res Express 9: 052001.

24. Raanaei H, Eskandari H, Mohammad-Hosseini V (2016) Structural and magnetic properties of nanocrystalline Fe–Co–Ni alloy processed by mechanical alloying. J Magn Magn Mater 398: 190–195.

25. Li X, Takahashi S (2000) Synthesis and magnetic properties of Fe–Co–Ni nanoparticles. J Magn Magn Mater 214: 195–203.

26. Zhou YJ, Zhang Y, Wang YL, Chen GL (2007) Microstructure and mechanical properties of AlxCoCrFeNi high-entropy alloys. Mater Sci Eng A 454–455: 260–265.

27. Senkov ON, Woodward C, Miracle DB (2014) Microstructure and properties of aluminum-containing refractory high-entropy alloys. JOM 66: 2030–2042.

28. Ye YF, Wang Q, Lu J, Liu CT, Yang Y (2020) Enhanced properties of AlxCoCrFeNi HEAs. J Alloys Compd 826: 154249.

29. Chang CH, Titus MS, Yeh JW (2018) Oxidation behaviour of refractory HEAs. Adv Eng Mater 20: 1700948.

30. Li Z, Pradeep KG, Deng Y, Raabe D, Tasan CC (2016) Metastable HEAs overcome strength-ductility trade-off. Nature 534: 227–230.

31. Chen Y, Li Z, Zhang Y (2020) Effect of Ti addition on FeCrNiMn HEA. Mater Sci Forum 982: 101–106.

32. Tong CJ, Lin SJ, Chen TL, Yeh JW (2019) Effect of Ti addition on AlxCoCrFeNi HEAs. J Alloys Compd 771: 275–282.

33. Wang Z, Gao MC, Liaw PK, Zhang Y (2019) Magnetic properties of high-entropy alloys. Entropy 21: 214.

34. Liu L, Zhu JB, Zhang C, Li JC, Jiang Q (2012) FeCoCuNiSnx HEAs. Mater Sci Eng A 548: 64–68.

35. Muangtong P, Rodchanarowan A, Chaysuwan D, Chanlek N, Goodall R (2020) Corrosion behaviour of CoCrFeNi-x alloys. Corros Sci 172: 108740.

36. Lutterotti L (2000) MAUD CPD. IUCr Newsletter 24.

37. Pungor E, Horvai G (1995) A Practical Guide to Instrumental Analysis.

38. Suryanarayana C, Ivanov E, Boldyrev VV (2001) Mechanical alloying science and technology. Mater Sci Eng A 304: 151–158.

39. Koch CC (2003) Top-down synthesis of nanostructured materials. Rev Adv Mater Sci 5: 91–99.

40. Hexagonal close packed structure (n.d.) ScienceDirect Topics. Available from

41. Yuge K, Ohta S (2018) Microscopic geometry rules ordering tendency in multicomponent alloys. arXiv.

42. Matsuura M, Rodriguez Vega M (2024) Golden ratio in quasicrystal vibrations. Phys 17: s121.

43. Nearly golden ratio order in Ta metallic glass (2020) Commun Phys 29: 046105.